Experimental Study of Temperature-Compensated Aluminum Nitride Lamb Wave Resonators

Chih-Ming Lin[1,2], Ting-Ta Yen[1,2], Yun-Ju Lai[1,2], Valery V. Felmetsger[3], Matthew A. Hopcroft[2], Jan H. Kuypers[2], and Albert P. Pisano[1,2]

[1]Department of Mechanical Engineering
University of California at Berkeley
Berkeley, CA, USA

[2]Berkeley Sensor and Actuator Center
University of California at Berkeley
Berkeley, CA, USA

[3]PVD Product Group
Tegal Corporation
San Jose, CA, USA

***Abstract*—In this paper, the temperature compensation of aluminum nitride (AlN) Lamb wave resonators using edge-type reflectors is experimentally studied and demonstrated. By adding one compensating silicon dioxide (SiO_2) layer with an appropriate thickness, the Lamb wave resonator can achieve a zero linear temperature coefficient of frequency (TCF). With the composite membranes including 1 µm AlN and 0.83 µm SiO_2, a Lamb wave resonator operating at 711 MHz exhibits a second-order TCF of –21.5 ppb/°C^2. The temperature-dependent frequency variation is less than 250 parts per million (ppm) over a wide temperature range from –55 °C to 125 °C. This temperature compensated AlN Lamb wave resonator is promising for future applications to thermally stable oscillators, filters, and sensors.**

Keywords–Piezoelectric Resonators, Lamb Wave Resonators, Aluminum Nitride, Silicon Dioxide, Temperature Compensation, Zero Linear TCF, RF MEMS.

I. INTRODUCTION

Frequency references with low phase noise and drift are important components for navigation systems, wireless communication systems, and signal processing applications. As is well known, crystal oscillators (XOs) and temperature compensated crystal oscillators (TCXOs) based on AT-cut quartz dominate this market because AT-cut quartz has outstanding performance of temperature and long-term stability. However, there are still some drawbacks and fabrication limitations of quartz based resonators. For example, quartz XOs operating in the GHz range are technically challenging because it is difficult to obtain uniform quartz plates of several micrometer thickness. In addition, the material property of quartz limits the integration of frequency references and CMOS circuits.

Therefore, in recent years AlN thin film attracts many MEMS researchers because it can provide a high acoustic phase velocity, small TCF, low motional resistance, and CMOS-compatible ability. Many RF MEMS studies focus on novel AlN-based resonators and filters, such as thin film plate acoustic resonators (FPAR) [1], contour-mode resonators [2, 3], and layered surface acoustic wave (SAW) filters [4]. Among these novel resonators, Lamb wave resonators based on AlN thin films are promising for higher frequency (several GHz) applications than SAW resonators because of the higher acoustic velocity. The lowest symmetric (S_0) mode Lamb wave of AlN has an acoustic velocity approaching 10,000 m/s, which is much higher than SAW velocity of about 4,000 m/s or S_0 mode $LiNbO_3$ Lamb wave velocity of about 6,000 m/s [5]. Furthermore, compared to other modes of Lamb waves, S_0 mode of Lamb waves shows the low dispersion which is beneficial for the fabrication tolerances towards thickness variations of the AlN layer [6].

However, similar to the thin film bulk acoustic resonators (FBAR) and the solid mounted resonators (SMR) using AlN thin films, the uncompensated Lamb wave resonator also has a linear TCF of –20 ppm/°C to –25 ppm/°C [6]. This level of temperature stability is unsuitable for any frequency reference applications. The temperature-frequency variation mainly results from material softening of these composite layers, such as AlN and Al when temperature increases. Fortunately, the thermal compensation technique of adding one compensating silicon dioxide layer can be used, which has been widely applied to different kinds of piezoelectric resonators [7-12] and silicon-based electrostatic MEMS resonators [13].

Recently, we have theoretically studied the temperature compensation of Lamb wave resonators using AlN/SiO_2 layered membrane [6]. In this work, we present the experimental studies of the temperature compensation of Lamb wave resonators. More specifically, we studied the

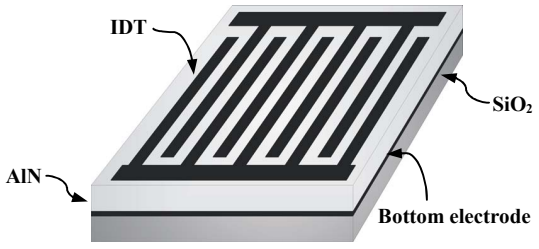

Figure 1. Illustration of the temperature-compensated AlN Lamb wave resonator using one compensating layer of silicon dioxide.

This work was supported by the DARPA M/NEMS S&T Fundamentals award (HR0011-06-1-0041) under the DARPA Center for Micro/Nano Scaling-Induced Physics (MiNaSIP).

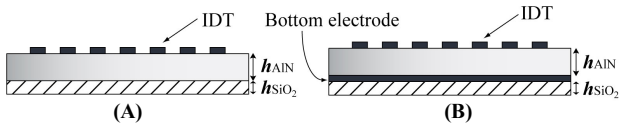

Figure 2. Cross-sectional view of two fundamental configurations for zero linear TCF AlN Lamb wave resonators using one SiO_2 layer.

temperature compensation of a Lamb wave resonator using edge-type reflectors. As shown in Figure 1, the Lamb wave resonator using edge-type reflectors is on the composite AlN/SiO_2 membranes. By designing the correct ratio of AlN thickness and SiO_2 thickness, a zero linear TCF Lamb wave resonator is experimentally demonstrated. The temperature-compensated Lamb wave resonator exhibits a quadratic temperature behavior at which the frequency is less sensitive to small temperature changes.

II. Lamb Wave in AlN/ SiO_2 Composite Membranes

A. Dispersion of Velocity & Electromechanical Coupling

The dispersive characteristics of an AlN/SiO_2 are studied by using Alder's approach [14]. The epitaxial relationships are that the (002) plane of AlN is parallel to the SiO_2 surface, the Lamb wave propagates in the plane normal to the *c*-axis of AlN thin film. We discuss two different configurations of AlN Lamb wave resonators using silicon dioxide as the compensating material as shown in Figure 2. In Figure 3, the solid lines and the dash lines represent the S_0 mode Lamb wave dispersion of the phase velocity and electromechanical coupling, respectively. On the other hand, the solid line and dash line represent the configuration (A), and the solid line with dot and dash line with dot represent the configuration (B). As a result, configurations (A) and (B) exhibit almost the same velocity dispersion, but configuration (B) has the higher electromechanical coupling than configuration (A). Therefore, we studied the TCF of the configuration (B) because the higher electromechanical coupling is more promising for future applications.

B. Linear TCF of AlN Lamb Wave Resonators

The linear TCF of the Lamb wave resonator on AlN/SiO_2 layered membranes is computed based on the temperature dependent material constants listed in Table I [7] when the electrode mass loading effect is neglected. By the linear approximation, the temperature dependent stiffness coefficients is $C_{ij}(T_0)$ and density $\rho(T_0)$ can be defined as

$$C_{ij}(T) = C_{ij}(T_0)(1 + TC_{ij}\Delta T) \tag{1}$$

$$\rho(T) = \rho(T_0)\left[1 - (a_{11} + a_{22} + a_{33})\Delta T\right] \tag{2}$$

The thermal expansion is assumed to be along the plate thickness and plate length; thus, the TCF for the Lamb wave resonator is written as

$$\mathrm{TCF_{LWR}} = \frac{1}{v}\frac{\partial v}{\partial T} - \alpha_x \tag{3}$$

where the first term refers to the temperature dependence of the Lamb wave velocity which is computed for ΔT equal to

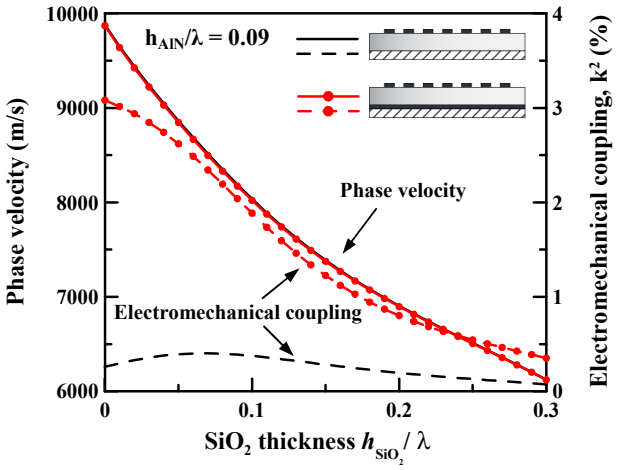

Figure 3. Lowest symmetric mode (S_0 mode) Lamb wave dispersion of phase velocity and electromechanical coupling in composite AlN/SiO_2 membranes.

10 K using all the temperature dependent parameters (TC_{ij}, α_z, ρ), and the thermal expansion along the propagation direction, α_x.

TABLE I. Temperature Coefficients of Material Constants [7]

	Symbol	AlN	Al	SiO_2
Temperature coefficient of elastic constants (10^{-4} °C^{-1})	TC_{11}	–0.37	–5.9	2.39
	TC_{12}	–0.018	–0.8	5.84
	TC_{13}	–0.018	–0.8	5.84
	TC_{33}	–0.65	–5.9	2.39
	TC_{44}	–0.5	–5.2	1.51
	TC_{66}	–0.57	–5.2	1.51
Thermal expansion coefficient (10^{-6} °C^{-1})	α_{11}	5.27	18	0.55
	α_{33}	4.15	18	0.55

As illustrated in Figure 4, an effective thermal expansion coefficient for estimating the elongation along the propagation direction of the Lamb wave device is required for computing the TCF of the composite structure. The effective thermal expansion for an arbitrary stack of layers is computed from the thermal expansion of the neutral plane in the stack [6]. The effective thermal expansion and the TCF of Lamb wave resonators for a stack of *i* layers with Young's modulus E_i, thickness t_i, and thermal expansion α_i, are then given as

$$\alpha_{\mathrm{eff}} = \frac{\sum_{i=1}^{n} E_i t_i \alpha_i}{\sum_{i=1}^{n} E_i t_i} \tag{4}$$

$$\mathrm{TCF_{LWR}} = \frac{1}{v}\frac{\partial v}{\partial T} - \alpha_{\mathrm{eff}} \tag{5}$$

The first-order TCF of Lamb wave resonators with configuration (B) is theoretically analyzed in this study. On AlN/SiO_2 composite structures, the linear TCF of Lamb wave with different AlN normalized thicknesses h_{SiO2}/λ of 0.05, 0.1,

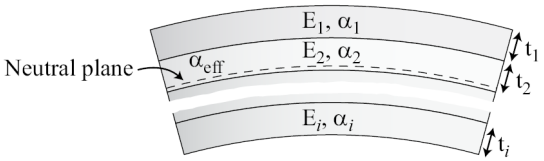

Figure 4. The effective thermal expansion experienced at the neutral plane is used for estimating the effective elongation in propagation direction.

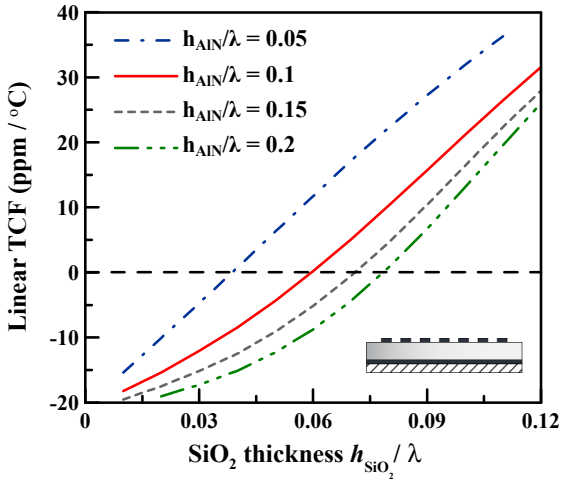

Figure 5. Dispersive characteristics of the linear TCF of Lamb wave resonators on AlN/SiO_2 composite structures.

0.15, and 0.2 are shown in Figure 5. The theoretical analysis shows the linear TCF of Lamb wave on AlN/SiO_2 composite membranes has dispersive characteristics. In other words, the first-order TCF is a function of relative SiO_2 thicknesses for different relative AlN thicknesses.

III. Fabrication Process

A five-mask process has been used to fabricate Lamb wave resonators. Low-stress nitride (LSN) and low temperature oxide (LTO) were first deposited on the silicon wafer. A 1 µm AlN film was sandwiched between a bottom aluminum electrode and a top aluminum electrode. Highly *c*-axis (002) oriented AlN films with FWHM of X-ray rocking curve 1.77 degree were deposited by ac reactive sputtering using Endeavor-AT sputter tool of Tegal Corporation. The top aluminum electrode and AlN thin film were patterned by Cl_2-based dry etching. During the dry etching process for AlN film, a LTO layer was deposited and used as the hard mask. CF_4-based dry etch process was used to remove the remaining LTO. Finally, the devices were released by XeF_2-based dry etching of silicon. Figure 6 shows the cross-sectional view of fabricated Lamb wave resonators which were fabricated by the above process. The stack of 1 µm thick AlN and 0.83 µm thick SiO_2 composite layers were used for the main structure of temperature-compensated Lamb wave devices in this study.

IV. Experimental Results and Discussion

The fabricated resonators were tested in a vacuum probe system (Suss MicroTec® PMC150) that allows probing of

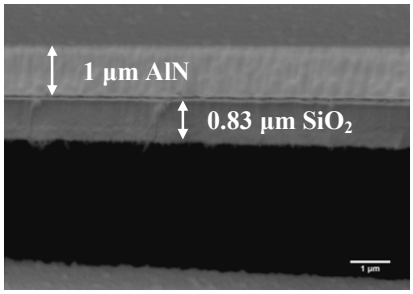

Figure 6. Cross-sectional view of a fabricated Lamb wave resonator on the stack of 1 µm AlN and 0.83 µm SiO_2 layers.

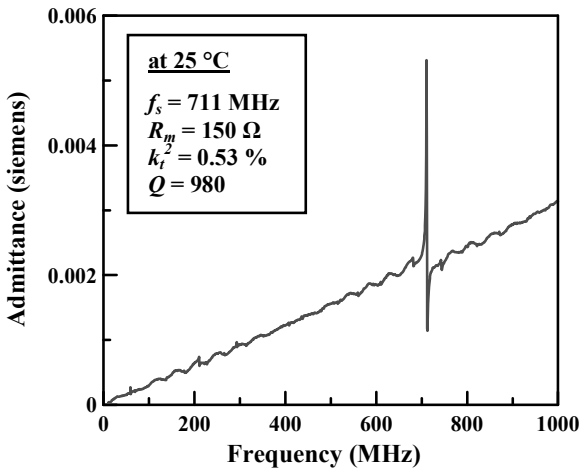

Figure 7. Measured frequency response of the zero linear TCF Lamb wave resonator (Design 2 in Table II).

chuck-mounted wafers while they are cooled via liquid helium or heated by electric heating elements (to the chuck). A feedback controlled heating unit provides a precise control of the chuck temperature during measurement. S_{11} parameters for resonators were extracted using an Agilent E8358A network analyzer. In order to measure the TCF for resonators, they were measured in the temperature range from –55 °C to 125 °C. The temperature was varied in 5 °C steps with 10 minute temperature stabilization before each measurement. Then the S_{11} parameters were logged five times for each 5 °C step and converted into equivalent admittances.

TABLE II. Dimensions of Lamb Wave Resonators

	Design 1	Design 2
Top electrode number	13	13
Aperture	125 µm	155 µm
Electrode width	4.44 µm	2.76 µm
Top electrode thickness	150 nm (Al)	150 nm (Al)
Bottom electrode thickness	150 nm (Al)	150 nm (Al)
AlN layer thickness	1 µm	1 µm
SiO_2 layer thickness	0.83 µm	0.83 µm

Figure 7 presents the measured frequency response of the Lamb wave resonator (Design 2 in Table II). This 711 MHz resonator shows a motional resistance of 150 Ω and a quality

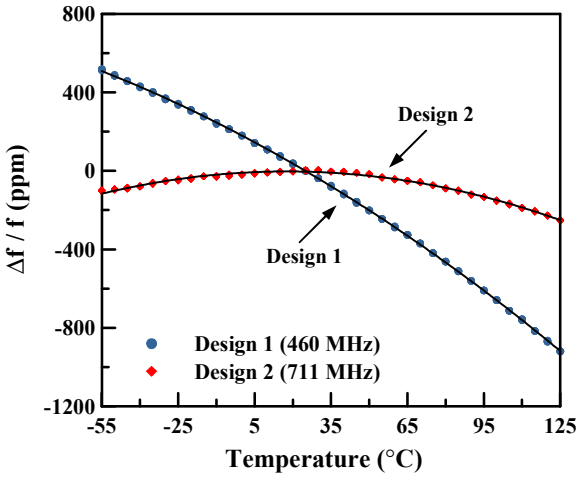

Figure 8. Measured frequency variation versus temperature of two thermally compensated AlN/SiO_2 Lamb wave resonators with different resonance frequencies.

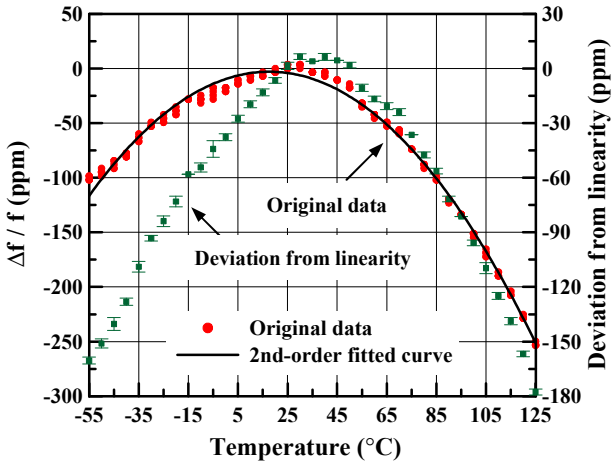

Figure 9. Measured frequency variation versus temperature of the thermally compensated AlN/SiO_2 Lamb wave resonator (Design 2). The deviation from linearity is used to extract the 2nd-order TCF.

factor of 980. It should be noted that there is no spurious mode over a 1 GHz frequency range which is excellent for the oscillator and filter applications. Fig. 8 shows the plot of measured frequency variation for two designs over a wide temperature range. Obviously, the temperature-dependent frequency variation of the two lamb wave resonators shows a quadratic function of temperature. As indicated in Table I, the first-order temperature coefficient of elastic constants of AlN and Al are negative, but SiO_2 has a positive temperature coefficient of elastic constants [7]. In other words, a stack of AlN, Al, and SiO_2 layers with an appropriate thickness ratio can zero out the linear TCF.

As pointed out in Figure 5, the first-order TCF is dispersive with the relative AlN thickness as well as the relative SiO_2 thickness. That is to say, the thickness ratio determines the TCF of the whole stacked structure. As shown in Figure 8, the first-order TCF of Design 1 resonator is not cancelled out since the ratio is not correct for this resonance frequency. Therefore, Design 1 resonator has a combination of first-order, second-order, and higher-order terms of TCFs and the first-order term dominates its characteristic of temperature-dependent frequency variation. For Design 1 resonator, its first-order term of TCFs is –7.9 ppm/°C and the second-order term is –15.6 ppb/°C^2.

With a proper combination of AlN and SiO_2, the linear TCF of Design 2 resonator is almost cancelled out so the second-order term dominates its characteristic of temperature-dependent frequency variation as shown in Figure 9. By subtracting the remaining linear part of TCF from the original data, the second-order TCF of –21.5 ppb/°C^2 is extracted as depicted in Figure 9. Thus, the frequency variation of the resonator exhibits a temperature-dependent quadratic function with a turnover temperature (T_M) and the frequency variation can be expressed as (β = –21.5 ppb/°C^2)

$$\frac{f(T)-f(T_M)}{f(T_M)} \approx \beta \times (T-T_M)^2 \qquad (6)$$

In the case of Design 2, the excellent temperature compensation of Lamb wave resonator was demonstrated with 0.83μm SiO_2 ($h_{SiO2}/\lambda = 0.075$) and 1 μm AlN ($h_{AlN}/\lambda = 0.0905$). The experimental results show good agreement with the theoretical predictions in Figure 5. It should be pointed out that although the two resonators were fabricated on the same wafers, the thin film deposition (AlN, Al, and SiO_2) was not ideally uniform on the whole wafer. On the other hand, the films showed the residual stresses of several hundred MPa. Therefore, the slight difference on the first-order TCF between theoretical simulation and experimental data might be the result of the non-uniformity of thin films [15] as well as the residual stresses. For more accurate prediction of the first-order TCF, the residual stresses have to be taken into account in the simulation [16].

V. Conclusion

In conclusion, Lamb wave resonators utilizing the lowest symmetric mode (S_0 mode) on AlN thin films can readily achieve the several GHz ranges because of its high acoustic velocity approaching 10,000 m/s. Compared to grating-based Lamb wave resonators, the edge-type reflectors can efficiently reduce the resonator size without sacrificing high quality factors. In this work, we have experimentally demonstrated that aluminum nitride Lamb wave resonators using edge-type reflectors can be temperature-compensated and achieve a zero first-order TCF by adding a layer of silicon dioxide with appropriate thickness since silicon dioxide has unique positive thermal coefficients of elastic constants. A temperature-compensated Lamb wave resonator operating at 711 MHz exhibits a second-order TCF of –21.5 ppb/°C^2, a motional resistance of 150 Ω, and a quality factor of 980. This second-order TCF of –21.5 ppb/°C^2 is close to the thermally compensated FBAR with –20 ppb/°C^2 [8] and smaller than the temperature-compensated FPAR with –31 ppb/°C^2 [11]. This technology is very promising to achieve oscillators and filters with CMOS compatible integration, low motional resistance, small size, and thermal stability.

ACKNOWLEDGMENT

The authors would like to acknowledge the help on AlN deposition from Dr. Shawn Tanner at Tegal Corporation and the help on Suss MicroTec® PMC150 probe system setup from Professor Clark T.-C. Nguyen's research group at UC Berkeley.

REFERENCES

[1] V. Yantchev, and I. Katardjiev, "Micromachined thin film plate acoustic resonators utilizing the lowest order symmetric Lamb wave mode," *IEEE Trans. Ultrason. Ferroelect. Freq. Contr.*, Vol. 54, pp. 87-95, 2007.

[2] G. Piazza, P. J. Stephanou, and A. P. Pisano, "Piezoelectric aluminum nitride vibrating contour-mode MEMS resonators," *J. Microelectromech. Syst.*, Vol. 15, pp. 1406-1418, 2006.

[3] P. J. Stephanou and A. P. Pisano, "GHz contour extensional mode aluminum nitride resonators," in *Proc. IEEE Intl. Ultrason. Symp.*, pp. 2401-2404, 2006.

[4] C.-M. Lin, Y.-Y. Chen, and T.-T. Wu, "A novel weighted method for layered SAW filters using slanted finger interdigital transducers," *J. Phys. D: Appl. Phys.*, Vol. 39, pp. 466-470, 2006.

[5] M. Kadota, T. Ogami, K. Yamamoto, Y. Negoro, and H. Tochishita, "High frequency Lamb wave device composed of $LiNbO_3$ thin film," in *Proc. IEEE Intl. Ultrason. Symp.*, pp. 1940-1943, 2008.

[6] J. H. Kuypers, C.-M. Lin, G. Vigevani, and A. P. Pisano, "Intrinsic temperature compensation of aluminum nitride Lamb wave resonators for multiple-frequency references," in *Proc. IEEE Int. Freq. Contr. Symp.*, pp. 240-249, 2008.

[7] J. Bjurstrom, G. Wingqvist, V. Yantchev, and I. Katardjiev, "Temperature compensation of liquid FBAR sensors," *J. Micromech. Microeng.*, Vol. 17, pp. 651-658, 2007.

[8] W. Pang, R. C. Ruby, R. Parker, P. W. Fisher, J. D. Larson III, K. J. Grannen, D. Lee, C. Feng, and L. Callaghan, "A thermally stable CMOS oscillator using temperature compensated FBAR," in *Proc. IEEE Intl. Ultrason. Symp.*, pp. 1041-1044, 2007.

[9] W. Pang, R. C. Ruby, R. Parker, P. W. Fisher, M. A. Unkrich, and J. D. Larson III, "A temperature-stable film bulk acoustic wave oscillator," IEEE Electron Device Lett., Vol. 29, pp. 315-318, 2008.

[10] S. Ohta, K. Nakamura, A. Doi, and Y. Ishida, "Temperature characteristics of solidly mounted piezoelectric thin film resonators," in *Proc. IEEE Intl. Ultrason. Symp.*, pp. 2011-2015, 2003.

[11] G. Wingqvist, L. Arapan, V. Yantchev, and I. Katardjiev, "A micromachined thermally compensated thin film Lamb wave resonator for frequency contorl and sensing applications," *J. Micromech. Microeng.*, Vol. 19, 035018, 2009.

[12] G. Wingqvist, L. Arapan, V. Yantchev, and I. Katardjiev, "Temperature compensation of thin AlN film resonators utilizing the lowest order symmetric Lamb mode," in *Proc. IEEE Intl. Ultrason. Symp.*, pp. 1207-1210, 2008.

[13] R. Melamud, B. Kim, S. A. Chandorkar, M. A. Hopcroft, M. Agarwal, C. M. Jha, and T. W. Kenny, "Temperature-compensated high-stability silicon resonators," *Appl. Phys. Lett.*, Vol. 90, 244107, 2007.

[14] A. A. Nassar and E. L. Adler, "Propagation and electromechanical coupling to plate modes in piezoelectric composite membranes," in *Proc. IEEE Int. Freq. Contr. Symp.*, pp. 369-372, 1983.

[15] M.-H. Chung, S. T. Wang, and A. C. S. Huang, "Study of frequency-temperature characteristics of quartz with various cut angle and metal thickness of electrode," in *Proc. IEEE Int. Freq. Contr. Symp.*, pp. 617-620, 2004.

[16] P. Nicolay, O. Elmazria, B. Assouar, F. Sarry, and L. Lebrizoual, "Theoretical and experimental study of the differential thermal expansion effect on the TCD of layered SAW temperature sensors," in *Proc. IEEE Intl. Ultrason. Symp.*, pp. 272-275, 2007.